POLITECNICO DI TORINO
Repository ISTITUZIONALE

3D-Printer-Based Test-Bench for Contactless Respiratory Monitoring Systems

Original
3D-Printer-Based Test-Bench for Contactless Respiratory Monitoring Systems / Pogliano, M., Buraioli, I., Sanginario, A., Demarchi, D., Ros, P.M.. - ELETTRONICO. - (2023), pp. -4. (IEEE Sensors conference 2023 Vienna (Austria) 29 October 2023 - 01 November 2023) [10.1109/SENSORS56945.2023.10325213].

Availability:
This version is available at: 11583/2985743 since: 2024-02-07T13:07:10Z

Publisher:
IEEE

Published
DOI:10.1109/SENSORS56945.2023.10325213

Terms of use:

This article is made available under terms and conditions as specified in the corresponding bibliographic description in the repository

Publisher copyright
IEEE postprint/Author's Accepted Manuscript

©2023 IEEE. Personal use of this material is permitted. Permission from IEEE must be obtained for all other uses, in any current or future media, including reprinting/republishing this material for advertising or promotional purposes, creating new collecting works, for resale or lists, or reuse of any copyrighted component of this work in other works.

(Article begins on next page)

05 November 2026

3D-Printer-Based Test-Bench for Contactless Respiratory Monitoring Systems

Marco Pogliano*, Irene Buraioli*, Alessandro Sanginario*, Danilo Demarchi* and Paolo Motto Ros*
*Dept. of Electronics and Telecommunications, Politecnico di Torino, Turin, Italy

***Abstract*—Respiratory monitoring is becoming an interesting research topic in many areas (health care, automotive, and aviation). One of the most prominent non-contact technologies is mm-wave radar, which allows real-time thoracic skin mm-movements tracking. The following work focuses on developing a test-bench to verify the performance of a breathing rate monitoring device based on a mm-wave radar. The innovative element of the setup concerns a 3D printer programmed by an automatic geometric code (G-code) generation tool that converts an ordered sequence of arbitrary temporal-position coordinates into a series of low-level instructions for reproducing the movement. A dielectric skin-equivalent dummy completes the test-bench and is used in the final stage to validate a 60 GHz radar-based system simulating respiratory displacement with physiological amplitudes and frequencies.**

***Index Terms*—3D printer, mm-wave radar, physiological remote monitoring, G-code generation tool, biomimetic movements**

I. Introduction

According to the latest report from the World Health Organization (WHO), the population is averagely aging with an increase in chronic diseases [1]. In these subjects, monitoring vital parameters, such as breathing rate, is clinically relevant to understanding the patient's state of health [2]. Moreover, COVID-19 has highlighted how respiratory disorders must be controlled in the presence of other pathologies [3].
In recent decades, devices capable of monitoring in real-time the breathing rate have increasingly been developed, classifiable as contact, wearable, or contactless [4]. Contact systems are based on electrodes (impedance analysis) [5], piezoelectric or piezoresistive sensors (respiratory belt) [6], or infrared radiation (plethysmography) [7]. They allow for reaching a high accuracy degree, but with several limitations, such as motion reduction, non-comfort conditions, possible allergic reactions, and disconnections [8], [9]. Over the years, wearable sensors based mainly on accelerometers [10] and photoplethysmography sensors [7] have been developed with the advantage of being integrated into smartwatches or bracelets. However, these devices' performance strongly depends on ambient light and skin contact conditions. Contactless imaging-based devices and radar-based systems have been investigated to overcome these limitations. Imaging-based devices can be thermal or optical, using thermal or RGB cameras with an AI elaboration [11]. Nevertheless, these systems highly depend on external lighting conditions; in this regard, radar-based devices can be a good solution. The operating mechanism is the following: a radio-frequency signal is emitted through a transmitter antenna, reflected by the target object, then the feedback signal is collected by the receiving antenna and processed to extract the needed information [9], [12]–[19].

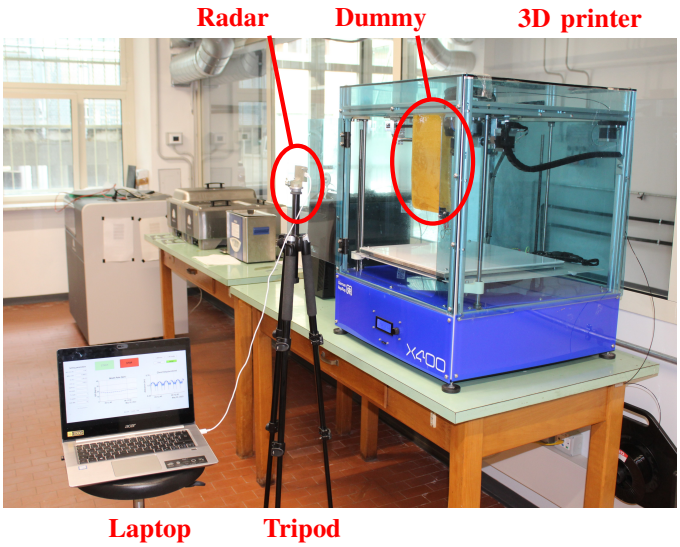


Fig. 1. 3D printer test-bench setup composed by a laptop connected via USB to the radar, the tripod to fix the inter-distance between radar and object, and the dummy hooked to the 3D printer rails.

These devices' design and the signal elaboration algorithm's development require numerous performance tests against a reference. Validations are often carried out as software simulations, on a custom test-bench, or on volunteer subjects. Software simulations used in the early stages of development often do not take into account the hardware in use by modeling an ideal case study. In [20], the corner reflector, designed to maximize radar reflections, is used as a target. However, this tool is inefficient for designing and testing a system capable of detecting chest mm-movements, as its geometrical properties are quite different from those of humans. In [21], [22], the test stages are performed directly on volunteer subjects by comparing the data with those derived from the gold standard, such as breathing belts. Reference measurements on volunteer subjects nevertheless require the control of many variables that could actually compromise the system's performance under validation, requiring calibration to the testing boundary conditions.
In this study, an innovative and unconventional test-bench, Fig. 1, is proposed. It comprises a 3D printer, reprogrammed using an automatic G-code generation tool to simulate biomimetic

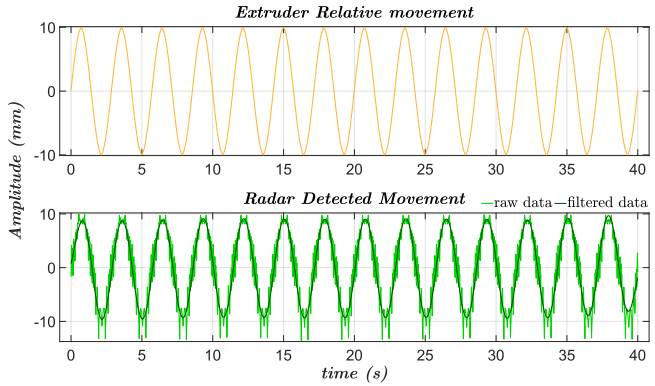


Fig. 2. 3D printer extruder relative movement compared to radar motion estimated movement.

respiratory movements by dynamically varying the phantom distance in real-time, and a skin-equivalent dielectric properties dummy used as the radar target. The flexibility of programmable motions and the high positioning accuracy of 3D printers make them excellent tools for this purpose. A specific test-bench has been developed and used to validate a system based on mm-wave radar and the complementary breathing frequency extraction algorithm as a proof-of-concept of the general test-bench architecture.

II. Material and Methods

The test-bench developed during this work consists of a dummy, a 3D filament printer, and an automatic G-code generation tool. The dummy, which reproduces the same dielectric characteristics as human skin at 60 GHz, the center-frequency of the specific radar, has been fabricated as presented in [23]. Following the proposed procedure, the semi-solid phantom has been made by weighing the different components using a high-precision balance (CPA225D, Sartorius). The water temperature has been measured with a thermocouple (FK26M, Test Product International). The mixture has then been poured into a flat-bottomed aluminum pan with dimensions of 20×30 cm, and a 3 mm-thick plywood panel has been placed over the mixture, allowing mechanical stability. To ensure the dielectric properties, the phantom thickness realized was approximately 8 mm, since the maximum penetration depth reached by a 60 GHz wave is about 0.5 mm [24]. The innovative element of the setup concerns the 3D printer. The printer choice is mainly constrained by the biomimetic movement characteristics to be reproduced; a common filament printer, the X400 from Germany's RepRap, was used in this project. Such a model has high accuracy in the extruder positioning (±100 µm). By means of two 3D-printed plastic supports the phantom was fixed on the extruder rails and oriented towards the radar. In this way, the extruder directly control the dummy along the radar-phantom axis. The thoracic motion simulation is performed by providing the 3D printer with G-code language commands. G-code is a programming language for computer numerical control machines. Each code line is a basic (low-level) instruction telling the machine what to do, where to move, how fast to move, and what path to follow. The G-code file is generated by a custom-developed MATLAB® tool, in which the input is an ordered sequence of arbitrary spatial and temporal coordinates. The algorithm processes consecutive time-position pairs, calculating the spatial and temporal differentials. From these two values, it computes the linear velocity required to accomplish the motion, considering the technical limitations specific to the printer. To overcome such limitations, which may be related to the maximum and minimum XY speeds, the algorithm implements iterative cycles to optimize input parameters, eventually taking advantage of strategic pause commands. The corresponding command, composed of the position to be achieved and velocity, is written into an external file containing the entire G-code instructions intended to reproduce the desired movement accurately.

This experimental setup has validated a respiratory frequency extraction system. Respiration can be divided into two phases (inhalation and exhalation) with different time supports due to the viscoelastic tissue response [25], [26]. In its simplified form, breathing can be modeled as a sinusoidal motion, neglecting its two phases' differences. Physiological thoracic respiration movements have an amplitude between 4 to 12 mm and a frequency range of 6 to 25 breaths per minute [27], [28]. Fig. 2 shows an example of the radar-detected motion compared to the programmed extruder movement.

The radar, which completes the specific setup tested, is mounted in a custom-made case and screwed on the tripod at the desired distance from the dummy. The case is fabricated with a resin 3D printer (FORM3+, Formlabs) to be mountable on a universal camera tripod. The radar used in the specific setup is the BGT60ATR24C provided by Infineon Technologies, programmed with a Graphical User Interface (GUI) on MATLAB®. The interface, via USB, allows setting the radar parameters, such as maximum working distance (0.96 m), spatial resolution (250 µm), sampling frequency (2.5 MHz), temporal parameters of the emitted wave, and power and gain parameters of the antennas. Once a breathing subject's presence is detected, chest motion and respiratory rate evaluations are shown on the interface. The developed algorithm processes

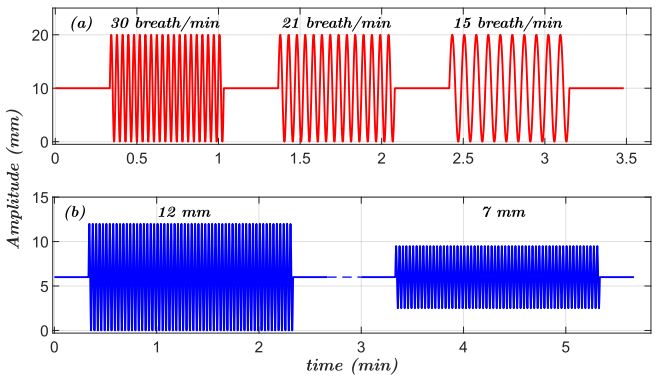


Fig. 3. (a) Frequency modulated burst signal example with an amplitude of 20 mm; (b) Physiological signal example with a frequency of 30 breaths/min.

TABLE I
FREQUENCY MODULATED BURST SIGNAL PARAMETERS AND BREATH RATE EVALUATED BY THE DEVICE.

Generated Frequency (breaths/min)	Generated Amplitude (mm)	Evaluated Frequency (breaths/min)	Error (%)
30	10	29.88 ± 0.01	-0.41
	20	29.69 ± 0.01	-1.02
	30	29.62 ± 0.23	-1.26
	40	29.04 ± 0.71	-3.18
21	10	21.02 ± 0.16	0.09
	20	20.81 ± 0.02	-0.89
	30	20.52 ± 0.41	-2.28
	40	20.78 ± 0.02	-1.05
15	10	14.83 ± 0.03	-1.11
	20	14.75 ± 0.03	-1.69
	30	14.71 ± 0.35	-1.90
	40	14.70 ± 0.09	-1.95
Average			-1.39

radar data in the frequency domain, extracting the object's instantaneous distance with a sampling rate of 2 kHz. The distance data from the last 20 s of the signal are filtered in the respiratory band (6 to 40 breaths per minute), and the breathing rate is evaluated with a frequency content analysis.

III. EXPERIMENTAL RESULTS AND DISCUSSION

The experimental setup validates a respiratory rate monitoring radar system by reproducing a lifelike respiratory movement of the flat dummy perpendicular to the radar. An actual physiological displacement (e.g., in tests involving human subjects) would have resulted in lower reference accuracy due to the significantly variable nature of consecutive breaths. Therefore, the respiratory model chosen is sinusoidal to have an exact frequency reference to validate the device accurately. Two different types of signals have been used in the testing stage. The first comprises three decreasing frequency bursts of about 40 s period with constant amplitude, interspersed with 20 s periods of inactivity. This one allows for evaluating the device's behavior at different respiratory frequencies. The signal amplitudes are kept wider than the physiological breathing to thoroughly analyze the radar data's correlation with the dummy's movement. Table I shows the wave parameters used during the tests. The second signal comprises a 20 s inactivity followed by a 2 min movement with constant amplitude and frequency and 20 s inactivity. This second type, simulating a respiratory pattern, aims to assess the accuracy of the system with reasonable physiological amplitudes under relaxed breathing ($\leq$25 breaths/min) or accelerated breathing ($>$25 breaths/min), which is harder to analyze. Table II shows the wave parameters used during the tests. Fig. 3 presents an example of both signals.

The system has been set up by placing the radar in the case and screwing on the tripod at 40 cm distance from the dummy. It has been connected via USB to a laptop and configured through a GUI. The acquisition started when the G-code designed with the tool was executed to reproduce the presented

TABLE II
PHYSIOLOGICAL SIGNAL PARAMETERS AND BREATH RATE EVALUATED BY THE DEVICE.

Generated Frequency (breaths/min)	Generated Amplitude (mm)	Evaluated Frequency (breaths/min)	Error (%)
35	4	34.96 ± 0.10	-0.10
30	7	30.05 ± 0.12	0.18
	12	29.91 ± 0.26	-0.30
24	7	24.12 ± 0.10	0.52
	12	24.12 ± 0.25	0.51
18	12	18.50 ± 1.06	2.77
Average			0.60

biomimetic signals. The first signal test is repeated five times for each amplitude. The estimated mean respiratory rate is calculated for each constant-frequency section. The five trials' mean values are averaged, and the standard deviation and the percentage error are calculated. The analysis of the results, Table I, shows how the test-bench allows evaluation of the system's responsiveness to the changes in respiratory rates. Tests for the second signal are repeated seven times for each combination, evaluating the same performance parameters as for the first. The results are shown in Table II.

The results obtained with the algorithm allow the evaluation of the proposed experimental setup at varying respiratory amplitudes and frequencies, precisely defined by the test-bench, removing all the boundary conditions typical of testing on volunteer subjects. The average percentage error obtained for stressful signals, Table I, is $-1.39\,\%$ while in lifelike amplitude conditions, Table II, it decreases to $0.6\,\%$.

IV. CONCLUSIONS

An unconventional use of a 3D printer with high positioning accuracy allowed the construction of a reliable test-bench to validate a remote breathing frequency monitoring system based on millimeter-wave radar. The proposed setup is adaptable to different printers and radars. The G-code generation tool that receives the motion's spatial and temporal coordinates from the user makes the test system highly flexible and programmable, open to support future tests based on pre-recorded or pre-designed signals, thus aiming at maximising the reproducibility and reliability of the test themselves. The test-bench has successfully validated a prototype breath rate detector under lifelike signals and stressful conditions. Future work will leverage this system to design new radar-based respiratory monitoring test-benches and validate new systems.

ACKNOWLEDGMENT

This work has been partially supported by the AI4CSM project inside the European H2020 research and innovation programme, ECSEL Joint Undertaking, under grant agreement No.101007326.

The authors thank Infineon Technologies, which supplied the BGT60ATR24C radar used to validate the designed test-bench.

REFERENCES

[1] E. Rudnicka, P. Napierała, A. Podfigurna, B. Meczekalski, R. Smolarczyk, and M. Grymowicz, "The World Health Organization (WHO) approach to healthy ageing," *Maturitas*, vol. 139, pp. 6–11, 2020.

[2] H. Zhang, S. Li, X. Jing, P. Zhang, Y. Zhang, T. Jiao, G. Lu, and J. Wang, "The separation of the heartbeat and respiratory signal of a doppler radar based on the lms adaptive harmonic cancellation algorithm," in *2013 Sixth International Symposium on Computational Intelligence and Design*, vol. 1. IEEE, 2013, pp. 362–364.

[3] Z. Zheng, F. Peng, B. Xu, J. Zhao, H. Liu, J. Peng, Q. Li, C. Jiang, Y. Zhou, S. Liu *et al.*, "Risk factors of critical & mortal COVID-19 cases: A systematic literature review and meta-analysis," *Journal of infection*, vol. 81, no. 2, pp. e16–e25, 2020.

[4] C. Massaroni, A. Nicolò, D. Lo Presti, M. Sacchetti, S. Silvestri, and E. Schena, "Contact-based methods for measuring respiratory rate," *Sensors*, vol. 19, no. 4, p. 908, 2019.

[5] F.-T. Wang, H.-L. Chan, C.-L. Wang, H.-M. Jian, and S.-H. Lin, "Instantaneous Respiratory Estimation from Thoracic Impedance by Empirical Mode Decomposition," *Sensors*, vol. 15, no. 7, pp. 16 372–16 387, 2015. [Online]. Available: https://www.mdpi.com/1424-8220/15/7/16372

[6] R. De Fazio, M. Stabile, M. De Vittorio, R. Velázquez, and P. Visconti, "An Overview of Wearable Piezoresistive and Inertial Sensors for Respiration Rate Monitoring," *Electronics*, vol. 10, no. 17, 2021. [Online]. Available: https://www.mdpi.com/2079-9292/10/17/2178

[7] S. A. Shah, S. Fleming, M. Thompson, and L. Tarassenko, "Respiratory rate estimation during triage of children in hospitals," *Journal of Medical Engineering & Technology*, vol. 39, no. 8, pp. 514–524, 2015.

[8] V. L. Petrović, M. M. Janković, A. V. Lupšić, V. R. Mihajlović, and J. S. Popović-Božović, "High-accuracy real-time monitoring of heart rate variability using 24 GHz continuous-wave Doppler radar," *Ieee Access*, vol. 7, pp. 74 721–74 733, 2019.

[9] D. Wang, S. Yoo, and S. H. Cho, "Experimental comparison of IR-UWB radar and FMCW radar for vital signs," *Sensors*, vol. 20, no. 22, p. 6695, 2020.

[10] G. B. Drummond, D. Fischer, M. Lees, A. Bates, J. Mann, and D. Arvind, "Classifying signals from a wearable accelerometer device to measure respiratory rate," *ERJ Open Research*, vol. 7, no. 2, 2021.

[11] F. Yang, S. He, S. Sadanand, A. Yusuf, and M. Bolic, "Contactless measurement of vital signs using thermal and RGB cameras: A study of COVID 19-related health monitoring," *Sensors*, vol. 22, no. 2, p. 627, 2022.

[12] E. Pittella, A. Bottiglieri, S. Pisa, and M. Cavagnaro, "Cardiorespiratory frequency monitoring using the principal component analysis technique on UWB Radar Signal," *International Journal of Antennas and Propagation*, vol. 2017, 2017.

[13] Y. Xiong, S. Chen, X. Dong, Z. Peng, and W. Zhang, "Accurate measurement in doppler radar vital sign detection based on parameterized demodulation," *IEEE Transactions on Microwave Theory and Techniques*, vol. 65, no. 11, pp. 4483–4492, 2017.

[14] M. Mercuri, P. J. Soh, G. Pandey, P. Karsmakers, G. A. Vandenbosch, P. Leroux, and D. Schreurs, "Analysis of an indoor biomedical radar-based system for health monitoring," *IEEE Transactions on Microwave Theory and Techniques*, vol. 61, no. 5, pp. 2061–2068, 2013.

[15] M. Zakrzewski, H. Raittinen, and J. Vanhala, "Comparison of center estimation algorithms for heart and respiration monitoring with microwave Doppler radar," *IEEE Sensors Journal*, vol. 12, no. 3, pp. 627–634, 2011.

[16] J. Weiß, R. Pérez, and E. Biebl, "Improved people counting algorithm for indoor environments using 60 GHz FMCW radar," in *2020 IEEE Radar Conference (RadarConf20)*. IEEE, 2020, pp. 1–6.

[17] M. Ali, A. Elsayed, A. Mendez, Y. Savaria, and M. Sawan, "Contact and remote breathing rate monitoring techniques: A review," *IEEE Sensors Journal*, vol. 21, no. 13, pp. 14 569–14 586, 2021.

[18] H. Liu, J. Allen, D. Zheng, and F. Chen, "Recent development of respiratory rate measurement technologies," *Physiological measurement*, vol. 40, no. 7, p. 07TR01, 2019.

[19] I. Costanzo, D. Sen, L. Rhein, and U. Guler, "Respiratory Monitoring: Current State of the Art and Future Roads," *IEEE Reviews in Biomedical Engineering*, vol. 15, pp. 103–121, 2022.

[20] A. Ahmad, J. C. Roh, D. Wang, and A. Dubey, "Vital signs monitoring of multiple people using a FMCW millimeter-wave sensor," in *2018 IEEE Radar Conference (RadarConf18)*. IEEE, 2018, pp. 1450–1455.

[21] M. Arsalan, A. Santra, and C. Will, "Improved contactless heartbeat estimation in FMCW radar via Kalman filter tracking," *IEEE Sensors Letters*, vol. 4, no. 5, pp. 1–4, 2020.

[22] J. Lee and S. K. Yoo, "Radar-based detection of respiration rate with adaptive harmonic quefrency selection," *Sensors*, vol. 20, no. 6, p. 1607, 2020.

[23] J. Lacik, V. Hebelka, J. Velim, Z. Raida, and J. Puskely, "Wideband skin-equivalent phantom for V-and W-band," *IEEE Antennas and Wireless Propagation Letters*, vol. 15, pp. 211–213, 2015.

[24] N. Chahat, M. Zhadobov, R. Sauleau, and S. I. Alekseev, "New method for determining dielectric properties of skin and phantoms at millimeter waves based on heating kinetics," *IEEE Transactions on Microwave Theory and Techniques*, vol. 60, no. 3, pp. 827–832, 2012.

[25] G. Paterniani, D. Sgreccia, A. Davoli, G. Guerzoni, P. Di Viesti, A. C. Valenti, M. Vitolo, G. M. Vitetta, and G. Boriani, "Radar-based monitoring of vital signs: A tutorial overview," 2022.

[26] A. R. Carvalho and W. A. Zin, "Respiratory system dynamical mechanical properties: modeling in time and frequency domain," *Biophysical reviews*, vol. 3, pp. 71–84, 2011.

[27] G. Shafiq and K. C. Veluvolu, "Surface chest motion decomposition for cardiovascular monitoring," *Scientific reports*, vol. 4, no. 1, p. 5093, 2014.

[28] X. Yang, G. Sun, and K. Ishibashi, "Non-contact acquisition of respiration and heart rates using Doppler radar with time domain peak-detection algorithm," in *2017 39th Annual International Conference of the IEEE Engineering in Medicine and Biology Society (EMBC)*. IEEE, 2017, pp. 2847–2850.